

High-pressure investigations of yttrium(III) oxoarsenate(V): Crystal structure and luminescence properties of Eu^{3+} -doped scheelite-type $\text{Y}[\text{AsO}_4]$ from xenotime-type precursors

Florian Ledderboge^a, Jan Nowak^a, Hans-Joachim Massonne^b, Katharina Förg^c,
Henning A. Höpfe^c, Thomas Schleid^{a,*}

^a Institute of Inorganic Chemistry, University of Stuttgart, Pfaffenwaldring 55, 70569 Stuttgart, Germany

^b Institute of Mineralogy and Crystal Chemistry, University of Stuttgart, Azenbergstraße 18, 70174 Stuttgart, Germany

^c Institute of Physics, University of Augsburg, Universitätsstraße 1, 86159 Augsburg, Germany

1. Introduction

The first reported ternary rare-earth metal(III) oxoarsenate(V) with the composition $RE[\text{AsO}_4]$ was in 1934 the yttrium compound $\text{Y}[\text{AsO}_4]$ [1] in the xenotime-type structure crystallizing tetragonally with space group $I4_1/amd$. Thus its structure has to be identical with the one of the mineral chernovite $RE[\text{AsO}_4]$ (RE : mainly Y and Ce) [1]. The xenotime-type structure is known for all oxoarsenates(V) $RE[\text{AsO}_4]$ containing rare-earth metals with small cationic radii ($RE = \text{Sc}, \text{Y}, \text{Sm} - \text{Lu}$) [1–11] and became named after the rare-earth metal(III) oxophosphate(V) mineral xenotime $RE[\text{PO}_4]$ (RE : mainly Y and Yb) [1], which shows the same structural arrangement as the mineral zircon $\text{Zr}[\text{SiO}_4]$ [12]. The oxoarsenates(V) $RE[\text{AsO}_4]$ with lighter and larger rare-earth metal(III) cations ($RE = \text{La} - \text{Nd}$) crystallize in the

monoclinic monazite-type structure (space group: $P2_1/n$) [1–4,13], also named after the isotypical rare-earth metal(III) oxophosphate(V) mineral monazite $RE[\text{PO}_4]$ ($RE = \text{mainly La and Ce}$) [14]. A high-pressure phase transition to the tetragonal scheelite-type crystal structure in space group $I4_1/a$ was reported for most of the rare-earth metals ($RE = \text{Y}, \text{La} - \text{Nd}, \text{Sm}, \text{Tb}, \text{Dy}, \text{Er}, \text{Yb}, \text{Lu}$) [15–18] in their oxoarsenates(V) $RE[\text{AsO}_4]$ referring to the isotypic mineral scheelite ($\text{Ca}[\text{WO}_4]$) [19]. The phase transition for the yttrium compound into the scheelite-type structure should start at 8 GPa and be completed at 12 GPa as found for the natural chernovite material ($\text{Y}[\text{AsO}_4]$ with 0.8% La and 0.6% P) [15]. Both tetragonal structures share eightfold oxygen coordination spheres (C.N. = 8) for the RE^{3+} cation, whereas the monoclinic monazite-type offers a coordination number of nine. Besides the oxoarsenates(V), oxoarsenates(III) of the rare-earth metals

* Corresponding author.

E-mail address: schleid@iac.uni-stuttgart.de (T. Schleid).

could also be synthesized. Here the compositions $RE_4[As_2O_5]_2[As_4O_8]$ ($RE = Nd$ and Sm) [20,21] were the first known rare-earth metal(III) oxoarsenates(III), followed by $RE[AsO_3]$ ($RE = La$ and Ce) crystallizing in the α - $Pb[SeO_3]$ - and the high-pressure $K[ClO_3]$ -type structures [17,22–24]. Furthermore, different derivatives of these oxoarsenates(III) with isolated $[AsO_3]^{3-}$ units were reported, which contain additional anions like chloride ($RE_5Cl_3[AsO_3]_4$ ($RE = La, Pr$ and Nd) [25,26]) as well as both oxide and halide ($RE_3OCl[AsO_3]_2$ ($RE = La, Ce, Gd$ and Tb) [27,28], $La_3OBr[AsO_3]_2$ [29], and $RE_5O_4Cl[AsO_3]_2$ ($RE = Pr$ and Nd) [30,31]), stemming from the halide fluxes of flux-assisted growth experiments for single crystals of the composition $RE[AsO_3]$.

2. Experiments, materials and methods

The precursor of yttrium(III) oxoarsenate(V) $Y[AsO_4]$ in the xenotime type was prepared by dissolving yttrium sesquioxide (Y_2O_3 : 99.9%, ChemPur, Karlsruhe, Germany) in nitric acid (HNO_3 : 13%, Scharr, Stuttgart, Germany) under stirring and heating. A stoichiometric amount of dissolved arsenic(V)-oxide hydrate ($As_2O_5 \cdot 3H_2O$: 99%, Merck, Darmstadt, Germany) was added to this solution, which finally became neutralized dropwisely with 1 M caustic soda (as aqueous solution of $NaOH$). A permanent precipitation was observed at a pH value of six, completed at $pH = 7$. The product was washed with demineralized water and dried at $100^\circ C$ for 3 h. For the Eu^{3+} -doped compound a small amount of europium sesquioxide (Eu_2O_3 : 99.9%, ChemPur, Karlsruhe, Germany) was directly added to the yttrium sesquioxide before its dissolution in nitric acid. As expected the crystallinity of the synthesized compounds was very poor and the X-ray powder diffraction (XRPD) patterns recorded with a STADI-P (STOE & Cie GmbH, Darmstadt, Germany) combined with a IP-PSD detector (STOE & Cie GmbH, Darmstadt, Germany) showed only broad peaks (Fig. 1). The heat treatment of the xenotime-type compound $Y[AsO_4]$ led to an enhanced crystallinity, as well as the subsequent high-pressure experiment for the formation of scheelite-type $Y[AsO_4]$.

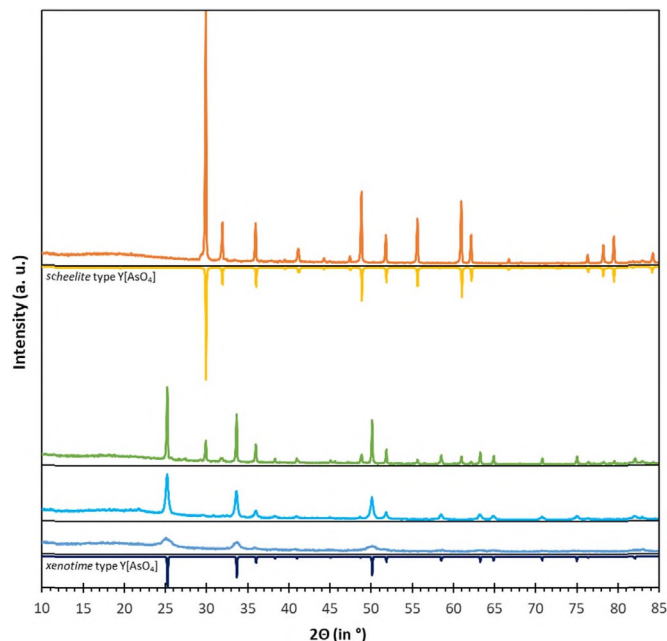


Fig. 1. X-ray powder diffraction patterns of the untreated xenotime-type $Y[AsO_4]$ (blue), samples after heating up to $850^\circ C$ and cooled down slowly (cyan), xenotime- and scheelite-type $Y[AsO_4]$ after a high-pressure experiment of 18 h (green) and pure scheelite-type $Y[AsO_4]$ after a high-pressure treatment of 44 h (orange) compared to theoretical patterns of $Y[AsO_4]$ xenotime-type (dark blue) and the scheelite-type $Y[AsO_4]$ (yellow). (For interpretation of the references to color in this figure legend, the reader is referred to the web version of this article.)

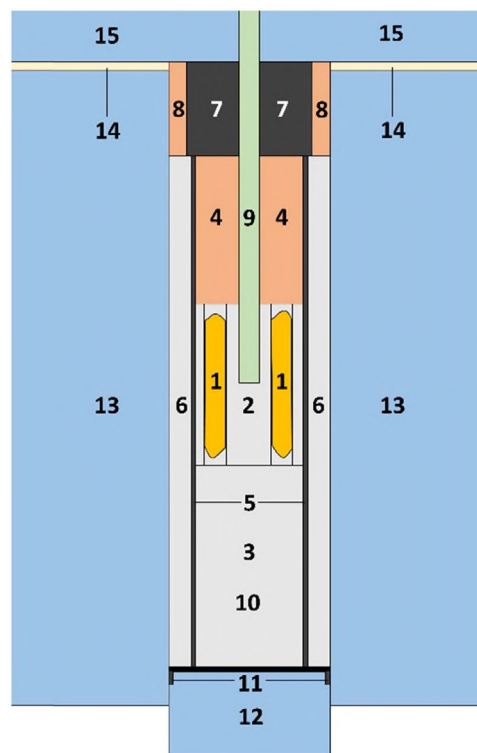


Fig. 2. Arrangement of the various components in the WC pressure cell used for the high-pressure experiments.

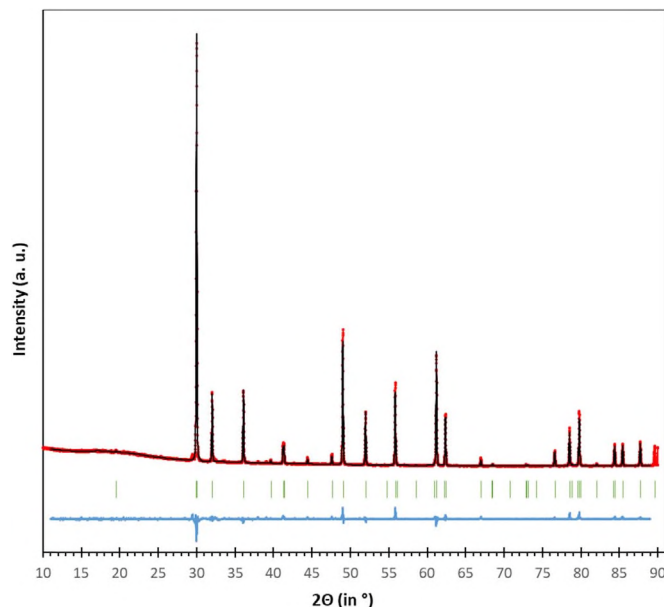


Fig. 3. Rietveld refinement (black line) in the range of $11^\circ \leq 2\theta \leq 89^\circ$ of a $Y[AsO_4]:Eu^{3+}$ powder pattern (red dots) including Bragg positions (green bars) and difference $Y_{obs} - Y_{calc}$ (blue line). (For interpretation of the references to color in this figure legend, the reader is referred to the web version of this article.)

For this experiment the untreated, just dried xenotime-type precursor powder was filled into small gold ampoules with a diameter of 2 mm and a length of 10 mm, which were sealed under atmospheric conditions with an arc welder. The filled ampoules before and after the high-pressure treatment were identified by their weight. These experiments were achieved in a piston-cylinder apparatus using a WC vessel with a pressure chamber of $1/2$ in. diameter (Fig. 2). Four gold ampoules (1) were put into a cylindrical, 4 cm long, low-friction pressure cell (2) of pressed sodium chloride with four fitting recesses around a central hole

Table 1

Crystallographic data and structure refinement for both tetragonal polymorphs of Y[AsO₄].

Empirical formula	YAsO ₄	
Structure type	Xenotime	Scheelite
Crystal system	tetragonal	
Space group	<i>I</i> 4 ₁ / <i>amd</i> (no. 141)	<i>I</i> 4 ₁ / <i>a</i> (no. 88)
Relative molar mass, <i>M_r</i>	227.83	
Lattice parameters: <i>a</i> , pm	704.63(6)	498.23(4)
<i>c</i> , pm	628.94(5)	1120.71(9)
<i>c/a</i>	0.893	2.249
Molar volume (<i>V_m</i> , cm ³ mol ⁻¹)	47.01	41.88
Number of formula units (<i>Z</i>)	4	
Calculated density (<i>D_x</i> , g cm ⁻³)	4.846	5.440
F(000)	416	
Absorption coefficient (<i>μ</i> (MoKα), mm ⁻¹)	29.013	32.567
<i>hkl</i> range	-9 ≤ <i>h</i> ≤ 9 -9 ≤ <i>k</i> ≤ 9 -8 ≤ <i>l</i> ≤ 8	-6 ≤ <i>h</i> ≤ 6 -6 ≤ <i>k</i> ≤ 6 -14 ≤ <i>l</i> ≤ 14
Collected reflections	2031	1621
Unique reflections	104	165
<i>R_{int}</i> / <i>R_σ</i>	0.040 / 0.014	0.091 / 0.049
Refined parameters	12	
<i>R₁</i> / <i>wR₂</i> (for all reflections)	0.015 / 0.030	0.053 / 0.075
Goodness of Fit (GoF)	1.070	0.928
Δρ _{min} (min/max), e ⁻ · 10 ⁻⁶ · pm ⁻³	-0.32 / 0.35	-0.638 / 0.672
Extinction coefficient, 10 ⁻⁶ · pm ⁻³	0.031(2)	0.004(1)
CSD numbers ^a	432,488	432,487
Radiation	Mo-Kα (λ = 71.07 pm)	
Instrument	κ-CCD (Bruker-Nonius)	
Structure solution and refinement	SHELX 2013 [42]	

^a Further details of the crystal structure investigations may be obtained from FIZ Karlsruhe, 76344 Eggenstein-Leopoldshafen, Germany (fax: (+49)7247-808-666; e-mail: crysdata(at)fiz-karlsruhe(dot)de, on quoting the given deposition numbers.

Table 2

Atomic positions and equivalent isotropic displacement parameters^a for both tetragonal polymorphs of Y[AsO₄].

Atom	Site	<i>x</i> / <i>a</i>	<i>y</i> / <i>b</i>	<i>z</i> / <i>c</i>	<i>U_{eq}</i> / pm ²
Xenotime-type Y[AsO₄]					
Y	4 <i>a</i>	0	3/4	1/8	98(3)
As	4 <i>b</i>	0	1/4	3/8	100(3)
O	16 <i>h</i>	0	0.4311(3)	0.2009(3)	173(6)
Scheelite-type Y[AsO₄]					
Y	4 <i>b</i>	0	1/4	5/8	137(5)
As	4 <i>a</i>	0	1/4	1/8	137(6)
O	16 <i>f</i>	0.2482(9)	0.1040(9)	0.4528(4)	154(9)

^a $U_{eq} = \frac{1}{3} (U_{11} + U_{22} + U_{33})$ [43,44].

for the sensor of the chromel-alumel thermocouple (9) to monitor and regulate the temperature within the furnace. The bottom is locked by a massive piece of sodium chloride (3), while the space in the cylinder is filled with fine powder of sodium chloride. A segment of calcinated pyrophyllite (4) is joining to the top also prepared with a drilling for the thermosensor. All these parts are put into a furnace of steel surrounded again by pressed sodium chloride (5,6). A base plug of steel cased by pyrophyllite (7,8) above and a platelet of carbon, a ring of steel and a piston (10–12) at the lower end finish the internals and are put into the high-pressure cell of tungsten carbide and mica (13–15) including an external water cooling system.

As far as possible the same conditions were chosen for both experiments to obtain the high-pressure phase of Y[AsO₄] and Y[AsO₄]:Eu³⁺, only the reaction time was increased. While the treatment with a pressure of 20 kbar at 700 °C within errors of ± 1 kbar and ± 20 °C for the ampoules filled with undoped yttrium(III) oxoarsenate(V) lasted only 18 h, the time for the Eu³⁺-doped compounds was increased to 44 h. A higher quality of crystallinity was observed for all samples after the high-pressure treatment, but only the

— 5 —

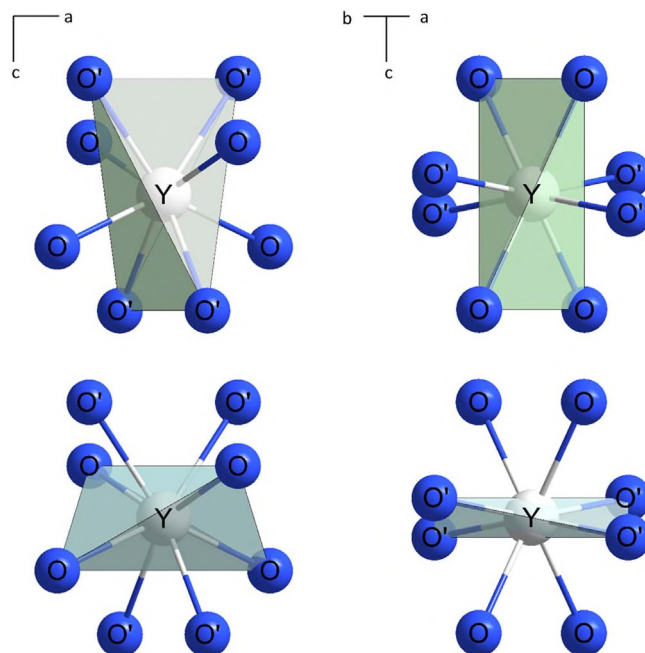


Fig. 4. Comparison of the trigonal dodecahedra of oxygen atoms surrounding the Y³⁺ cations described as interpenetrating prolated (*top*) and oblated tetrahedra (*bottom*) in the scheelite-type (*left*) and the xenotime-type crystal structure of Y[AsO₄] (*right*).

Table 3

Selected interatomic distances (*d*/pm) and angles (α/°) in both tetragonal polymorphs of Y[AsO₄].

Xenotime-type Y[AsO₄]		Scheelite-type Y[AsO₄]	
[YO ₈] ¹³⁻ polyhedron		[YO ₈] ¹³⁻ polyhedron	
Y – O	229.7(2) (4×)	Y – O	232.4(4) (4×)
Y – O'	241.4(2) (4×)	Y – O'	240.5(4) (4×)
[AsO ₄] ³⁻ tetrahedron		[AsO ₄] ³⁻ tetrahedron	
As – O	168.1(2) (4×)	As – O	169.2(4) (4×)
O – As – O	98.7(1) (2×)	O – As – O	105.4(1) (4×)
O – As – O	115.1(1) (4×)	O – As – O	118.0(3) (2×)

— 6 —

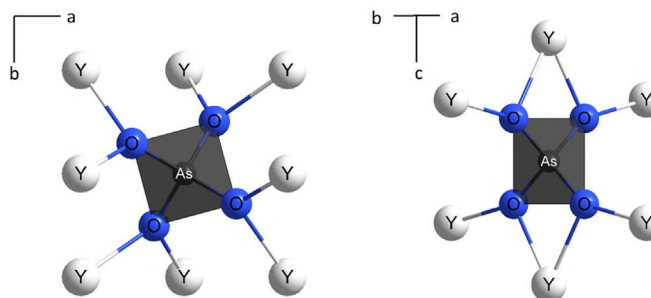


Fig. 5. Tetrahedral [AsO₄]³⁻ anion surrounded by eight Y³⁺ cations in the scheelite-type (*left*) and by six Y³⁺ cations in the xenotime-type structure of Y[AsO₄] (*right*).

longer lasting experiments with the europium(III)-doped compounds showed a complete phase-transition to the scheelite-type structure (Fig. 1). The experiments were stopped by switching off the heating, resulting in a temperature decrease to less than 100 °C within a minute. Afterwards the applied pressure was reduced to zero within 30 min. Contrary to our expectation only the undoped Y[AsO₄] exhibited larger single crystals up to 0.03 mm, measurable with a single-crystal X-ray

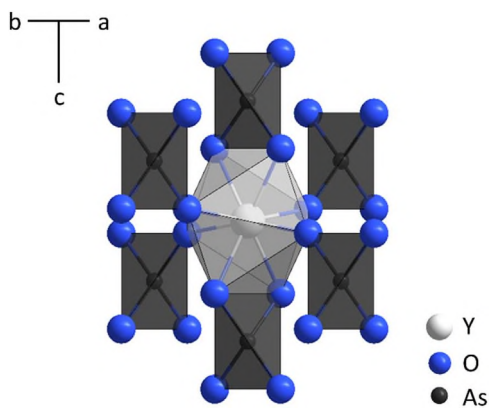


Fig. 6. Surrounding of the Y^{3+} cation by six $[AsO_4]^{3-}$ anions attached via vertices ($4\times$) and edges ($2\times$) in xenotime-type $Y[AsO_4]$.

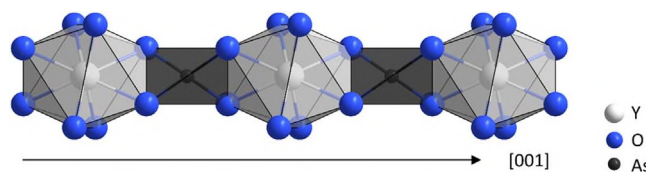


Fig. 7. Chain of alternating trigonal $[YO_8]^{13-}$ dodecahedra and $[AsO_4]^{3-}$ tetrahedra connected via *trans*-oriented edges propagating along $[001]$ in the xenotime-type structure of $Y[AsO_4]$.

diffractometer κ -CCD (Bruker-Nonius, Karlsruhe, Germany). A successful and still irreversible phase transition to the scheelite-type structure of yttrium(III) oxoarsenate(V) at a relatively low pressure of 20 kbar seems remarkable as it is just one sixth of the reported pressure for $Y[AsO_4]$ at room temperature, but in the same order of magnitude as for $Y[CrO_4]$ [15]. The samples of scheelite-type $Y[AsO_4]:Eu^{3+}$ were measured a STADI-P using a PSD detector (STOE & Cie GmbH, Darmstadt, Germany) and refined with Rietveld methods (Fig. 3).

3. Results and discussion

Crystallographic data and structure refinement parameters for the two $Y[AsO_4]$ dimorphs are given in Table 1. The atomic positions and

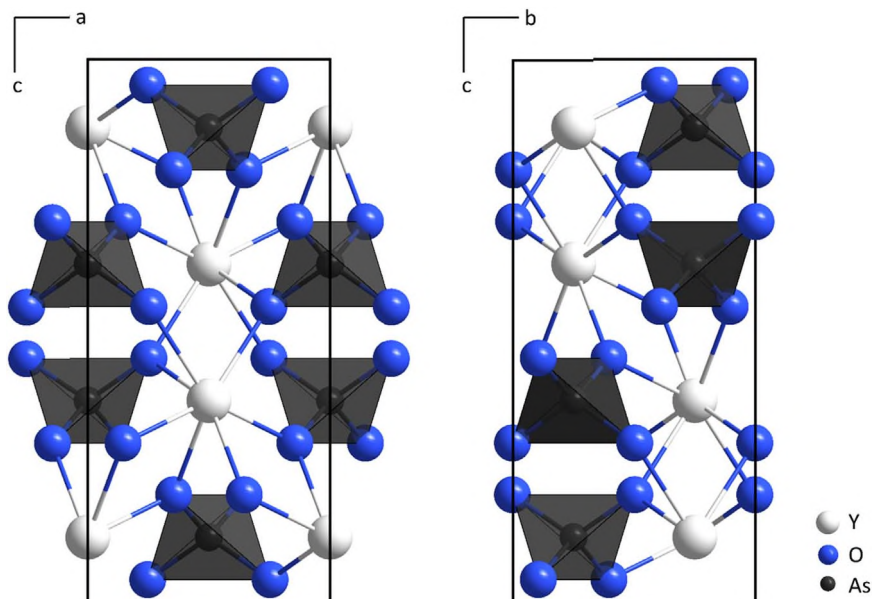


Fig. 8. Discrete $[AsO_4]^{3-}$ tetrahedra in the structure of scheelite-type $Y[AsO_4]$ as emphasized with views along $[010]$ (right) and $[100]$ (left).

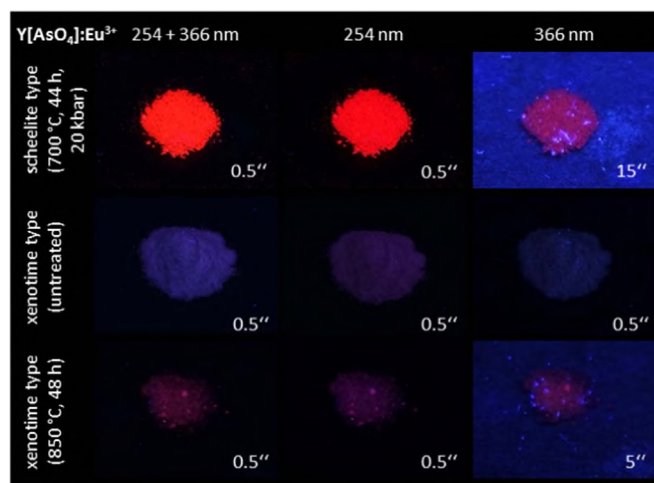


Fig. 9. Photographs of three samples of $Y[AsO_4]:Eu^{3+}$ under ultraviolet light with a wavelength of $\lambda = 254$ and/or 366 nm with the weakly luminous untreated precursor (*mid*) and samples of this precursor after a heat treatment at 850 °C for 48 h followed by a slow cooling (*bottom*) and after a high-pressure experiment (20 kbar) for 44 h at 700 °C (*top*).

equivalent isotropic displacement parameters are shown in Table 2. $Y[AsO_4]$ crystallizes in both cases tetragonally and shows the space group $I4_1/a$ with the lattice parameters $a = 498.23(4)$ and $c = 1120.71(9)$ pm for the scheelite-type and $I4_1/amd$ with the lattice parameters $a = 704.63(6)$ and $c = 628.94(5)$ pm for the xenotime-type structure with $Z = 4$ for both. In either structure the crystallographically unique Y^{3+} cations show an eightfold coordination with four *plus* four O^{2-} anions each in the shape of a trigonal dodecahedron with the respective fourfold distances $d(Y-O)_{\text{xenotime}} = 229.7(2)$ and $241.4(2)$ pm in the xenotime-type as well as $d(Y-O)_{\text{scheelite}} = 232.4(4)$ and $240.5(4)$ pm (Table 1) in the scheelite-type structure. Both polyhedra can be seen as a combination of two interpenetrating bisphenoidally distorted tetrahedra: one is prolated and the other one is oblated along $[001]$ (Fig. 4). In both cases the trigonal dodecahedra are connected to four adjacent $[YO_8]^{13-}$ polyhedra via shared edges. For the $[AsO_4]^{3-}$ units the four bond lengths between the As^{3+} cations and the O^{2-} anions are slightly shorter for the xenotime-type with $d(As-O)_{\text{xenotime}} = 168.1(2)$ pm as compared to the high-

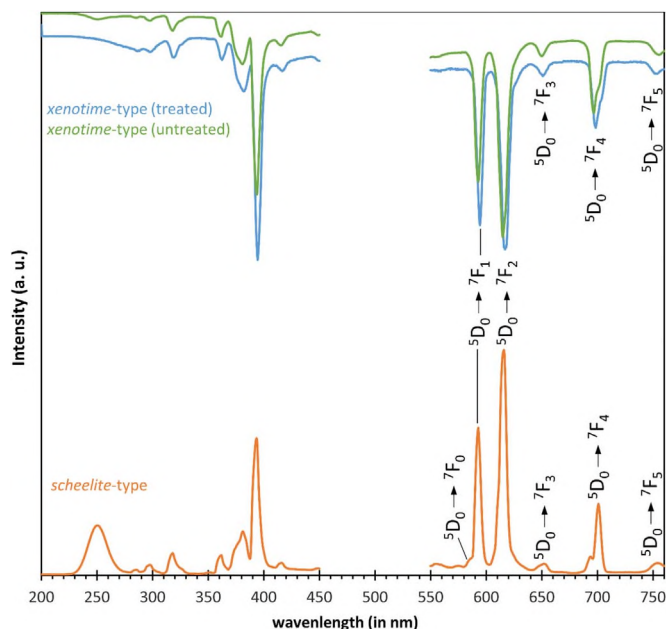


Fig. 10. Excitation spectra at 393 nm (left) and emission spectra at 616 nm (right) of both polymorphs (xenotime- and scheelite-type) of $Y[AsO_4]:Eu^{3+}$.

Table 4

Assignment of the $f-f$ transitions of untreated / treated xenotime-type and scheelite-type $Y[AsO_4]:Eu^{3+}$.

Transition	E (in eV)	$\bar{\nu}$ (in cm^{-1})	λ (in nm)
Xenotime-type $Y[AsO_4]$			
$^5D_0 \rightarrow ^7F_0$	Not detected		
$^5D_0 \rightarrow ^7F_1$	2.12 / 2.08	17,606 / 16,807	593 / 595
$^5D_0 \rightarrow ^7F_2$	2.02 / 2.01	16,260 / 16,207	615 / 617
$^5D_0 \rightarrow ^7F_3$	1.91 / 1.90	15,385 / 15,361	650 / 651
$^5D_0 \rightarrow ^7F_4$	1.78 / 1.77	14,347 / 14,306	697 / 699
$^5D_0 \rightarrow ^7F_5$	1.64 / 1.64	13,245 / 13,263	755 / 754
Scheelite-type $Y[AsO_4]$			
$^5D_0 \rightarrow ^7F_0$	2.12	17,606	586
$^5D_0 \rightarrow ^7F_1$	2.09	16,863	593
$^5D_0 \rightarrow ^7F_2$	2.01	16,234	616
$^5D_0 \rightarrow ^7F_3$	1.90	15,337	652
$^5D_0 \rightarrow ^7F_4$	1.77	14,265	701
$^5D_0 \rightarrow ^7F_5$	1.64	13,245	755

pressure scheelite-type structure with $d(As-O)_{\text{scheelite}} = 169.2(4)$ pm (Table 3). In addition, the angles $\angle(O-As-O)$ of the $[AsO_4]^{3-}$ anions get closer to the perfect tetrahedral angle, while moving from the xenotime-type structure ($\angle(O-As-O)_{\text{xenotime}} = 2 \times 98.7(1)$ and $4 \times 115.1(1)^\circ$) to the high-pressure polymorph ($\angle(O-As-O)_{\text{scheelite}} = 4 \times 105.4(1)$ and $2 \times 118.0(3)^\circ$). The arrangement of Y^{3+} cations surrounding the $[AsO_4]^{3-}$ anions changes from four terminal and two bridging cations in the xenotime-type to just eight terminal ones in the scheelite-type structure (Fig. 5). The pressure-distance paradoxon described by Kleber [34] can be observed for the average distances as well as the acceptance of the pressure-coordination rule by Neuhaus [35], because the number of coordinating $[AsO_4]^{3-}$ anions increases from six to eight, although the number of first-sphere coordinating oxygen atoms remains eight. Therefore, one of the eight oxygen atoms of the trigonal $[YO_8]^{13-}$ dodecahedron have to be connected by face or two of them have to share an edge with the $[AsO_4]^{3-}$ anion in the xenotime-type structure. Here, the latter is applied, as it can be seen in Fig. 6: the two opposite edges of the elongated disphenoid are linked by $[AsO_4]^{3-}$ anions and chains of alternating $[YO_8]^{13-}$ and $[AsO_4]^{3-}$ polyhedra propagate along [001] (Fig. 7) and dominate the structure of xenotime-type $Y[AsO_4]$. In contrast to that such an arrangement can not be found in the scheelite-type structure any more, as there is no

Table 5

Raman shifts ($\bar{\nu}/cm^{-1}$) of scheelite-type $Y[AsO_4]$ and xenotime-type $Y[AsO_4]$ recorded at $\lambda = 532$ nm compared with the minerals xenotime ($Y[PO_4]$) [41], scheelite ($Ca[WO_4]$) [40], and monazite ($Ce[PO_4]$) [39] (all with $\lambda = 532$ nm).

Scheelite-type $Y[AsO_4]$	Xenotime-type $Y[AsO_4]$	Xenotime ($Y[PO_4]$)	Scheelite ($Ca[WO_4]$)	Monazite ($Ce[PO_4]$)
				1070
		1056		1057
		1024	1028	1027
		999		989
				972
	896		910	
	887			
	843		837	
814				
788			747	
		689		
		663	660	
648	671		638	
	643			
611				621
		604		
575				590
			548	571
				536
		517		
	499			
			485	
	473	476		
467	463			466
			451	
439			436	
430				
		424		
412				415
404	399	406		396
		380	387	
379		375	373	373
343		338		
			333	
			310	
			297	
	279			277
275				
259	261			
		248	252	
233	238	232		
222	216			223
210	207			
196	184			
	168			
	145			

edge-sharing connection between the both oxygen polyhedra about the Y^{3+} and As^{5+} cations leading to a more complex vertex-shared arrangement (Fig. 8). Calculations of the Madelung Part of the Lattice Energy (MAPLE) [32,33] show that $Y[AsO_4]$ in the less dense xenotime-type (MAPLE = 6673 kJ mol^{-1}) exhibits a slightly smaller electrostatic part of the lattice energy than in the denser scheelite-type (MAPLE = 6711 kJ mol^{-1}). It is worth mentioning that our structural investigations confirm well the results and calculations of Errandonea and Sáez Puche et al. [15] for the natural mineral chernovite, if one keeps in mind that its lanthanum and phosphorus content develops slightly different lattice parameters. Moreover, another high-pressure phase transition can be achieved at pressures higher than 32 GPa resulting in the $SrUO_4$ -type structure [36,37] of $YAsO_4$, which no longer contains isolated $[AsO_4]^{3-}$ tetrahedra, but vertex-connected $[AsO_6]^{7-}$ octahedra forming layers according to $2_{\infty}^2([AsO_{4/2}O_{2/1}]^{3-})$ ($\nu \equiv$ vertex-connecting, $t \equiv$ terminal; $d(As-O)_{SrUO_4} = 172 - 188$ pm) held together by Y^{3+} cations in (9 + 1)-fold oxygen coordination ($d(Y-O)_{SrUO_4} = 220 - 252$ plus 288 pm) [15].

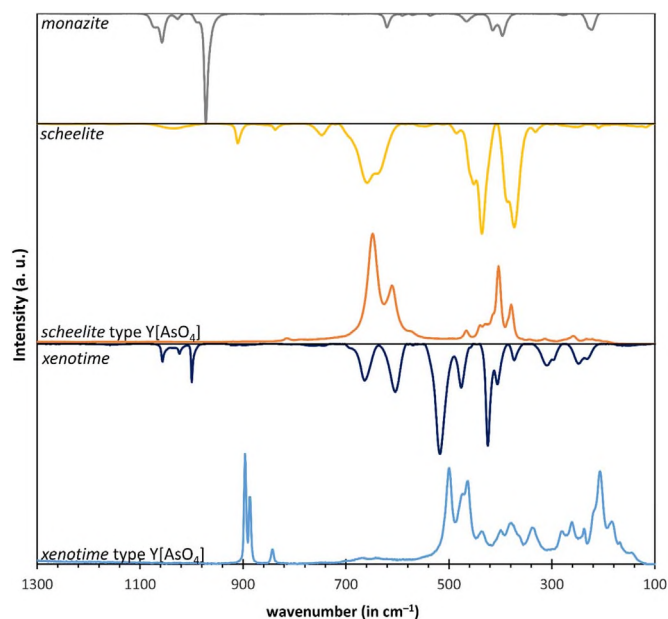


Fig. 11. Single-crystal Raman spectra of xenotime-type $\text{Y}[\text{AsO}_4]$ (blue) and scheelite-type $\text{Y}[\text{AsO}_4]$ (orange) as compared to the spectra of the minerals monazite ($\text{Ce}[\text{PO}_4]$, gray) [39], scheelite ($\text{Ca}[\text{WO}_4]$, yellow) [40] and xenotime ($\text{Y}[\text{PO}_4]$, dark blue) [41], all recorded at $\lambda = 532 \text{ nm}$. (For interpretation of the references to color in this figure legend, the reader is referred to the web version of this article.)

4. Spectroscopy

The visual comparison of the $\text{Y}[\text{AsO}_4]$ samples under UV light in a MinUVIS (Desaga, Wiesloch, Germany) revealed very clear results (Fig. 9). The untreated precursor of $\text{Y}[\text{AsO}_4]:\text{Eu}^{3+}$ with the xenotime-type structure exhibits only a very weak luminescence of blue to purple at both wavelengths used (254 and 366 nm), whereas the compound recrystallized at 850 °C in a CsBr flux already shows a greater portion of red light. The high-pressure phase $\text{Y}[\text{AsO}_4]:\text{Eu}^{3+}$ with the scheelite-type structure finally displays a bright, red luminescence at an excitation wavelength of $\lambda = 254 \text{ nm}$. However, a stimulation with a radiation of $\lambda = 366 \text{ nm}$ results in a diminished luminescence for all samples. These first impressions were excellently supported by luminescence measurements (Fig. 10) recorded with a FluoroMa6 (HORIBA Jobin Yvon, Bensheim, Germany). In the emission spectra of both polymorphs all $f-f$ transitions from ${}^5\text{D}_0$ to ${}^7\text{F}_J$ ($J = 1 - 5$) and for the scheelite-type phase also those from ${}^5\text{D}_0$ to ${}^7\text{F}_0$ were observed at the expected wavelength (Table 4). But in the excitation spectra there is a noticeable difference by a charge-transfer band, which is only observed in the high-pressure phase. This broad charge-transfer band of $\text{Y}[\text{AsO}_4]:\text{Eu}$ in the scheelite-type structure is located at 250.5 nm, which matches well with other oxoanionic europium(III) compounds like $\text{Eu}[\text{PO}_4]$ (231.5 nm) or $\text{Eu}_2[\text{SO}_4]_3$ (237.0 nm) [38].

Single-crystal Raman experiments were carried with an XploRA Raman microscope (HORIBA Jobin Yvon, Bensheim, Germany) for both yttrium(III) oxoarsenate(V) phases and exhibit a variety of different bands with wavenumbers between 100 and 900 cm^{-1} . The strongest bands of the xenotime-type phase are localized at 896, 887, 499, 463 and 207 cm^{-1} , whereas the main bands of the scheelite-type phase show up at different peaks (648, 611, 404 and 379 cm^{-1} , Table 5). The higher wavenumbers are each assigned to the symmetric and antisymmetric stretching modes and the lower ones to various deformation modes. The reason for the higher total amount and wider distribution range of vibrations bands in the xenotime-type compounds is caused by the different structural surrounding of the $[\text{AsO}_4]^{3-}$ units as compared to the simpler one in the scheelite-type phase (Fig. 11).

5. Conclusion

A new structure refinement of xenotime-type $\text{Y}[\text{AsO}_4]$ was achieved resulting in significant changes of several atomic distances as compared to the well-known mineral chernovite. The experimental data prove a high-pressure phase transition from xenotime- to scheelite-type yttrium(III) oxoarsenate(V) $\text{Y}[\text{AsO}_4]$ increasing its density D_x from 4.85 to 5.44 g cm^{-3} (that means by 12.2%). In addition, the excitation with ultraviolet light a bright red luminescence for the europium(III)-doped compound with the scheelite-type structure with a charge-transfer band located at 250.5 nm. As no such charge-transfer band was observed in the spectra of xenotime-type $\text{Y}[\text{AsO}_4]:\text{Eu}$, no luminescence in this range occurs here. The single-crystal Raman spectra exhibit the expected structure of bending modes for both polymorphs with wavenumbers below 900 cm^{-1} owing to vibrations of the discrete $[\text{AsO}_4]^{3-}$ anions.

Acknowledgements

We thank Dr. Falk Lissner for the X-ray single-crystal diffraction measurements and the State of Baden-Württemberg (Stuttgart) for the financial support of our research.

References

- [1] M. Strada, G. Schwendimann, *Gazz. Chim. Ital.* 64 (1934) 662–674.
- [2] D.-H. Kang, Th. Schleid, *Z. Anorg. Allg. Chem.* 631 (2005) 1799–1802.
- [3] A. Brahimi, M.M. Ftini, H. Amor, *Acta Crystallogr.* 58 (2002) 98–99.
- [4] M. Schmidt, U. Müller, R. Cardoso Gil, E. Milke, M. Binnewies, *Z. Anorg. Allg. Chem.* 631 (2005) 1154–1162.
- [5] F. Weigel, V. Scherrer, *Radiochim. Acta* 7 (1967) 46–50.
- [6] S. Golbs, R. Cardoso Gil, M. Schmidt, *Z. Krist.* 224 (2009) 169–170.
- [7] F.G. Long, C.V. Stager, *Can. J. Phys.* 55 (1977) 1633–1640.
- [8] W. Schäfer, G. Will, *J. Phys. C: Solid State Phys.* 4 (1971) 3224–3233.
- [9] D.-H. Kang, P. Höss, Th. Schleid, *Acta Crystallogr. E* 61 (2005) i270–i272.
- [10] G. Lohmüller, G. Schmidt, B. Deppisch, V. Gramlich, C. Scherfing, *Acta Crystallogr. B* 29 (1973) 141–142.
- [11] H.E. Swanson, M. Cook Morris, E.H. Evans, L. Ulmer, *Standard X-Ray Diffraction Powder Patterns*, U.S. Department of Commerce, National Bureau of Standards Monograph 25 – Section 3, Washington, DC (USA) 31–36 54–56.
- [12] W. Binks, *Mineral. Mag. J. Mineral. Soc.* 21 (1926) 176–187.
- [13] D.-H. Kang, *Doctoral Thesis*, Univ. Stuttgart, 2009.
- [14] M.P. Kokkoros, *Prakt. Akad. Athenon* 17 (1942) 163–174.
- [15] D. Errandonea, R. Kumar, J. López-Solano, P. Rodríguez-Hernández, A. Muñoz, M.G. Rabie, R. Sáez Puche, *Phys. Rev. B* 83 (2011) 134109-1–134109-12.
- [16] D.-H. Kang, Th. Schleid, *Z. Anorg. Allg. Chem.* 632 (2006) (2147–2147).
- [17] S.J. Metzger, *Doctoral Thesis*, Univ. Stuttgart, Stuttgart, 2012.
- [18] S.J. Metzger, F. Ledderboge, G. Heymann, H. Huppertz, Th. Schleid, *Z. Naturforsch.* 71 b (2016) 439–445.
- [19] R.G. Dickinson, *J. Am. Chem. Soc.* 42 (1920) 85–93.
- [20] D.-H. Kang, Th. Schleid, *Z. Anorg. Allg. Chem.* 632 (2006) 91–96.
- [21] M. Ben Hamida, C. Warns, M.S. Wickleder, *Z. Naturforsch.* 60 b (2005) 1219–1223.
- [22] F. Ledderboge, Th. Schleid, *Z. Krist. Suppl.* 34 (2014) (121–121).
- [23] S.J. Metzger, G. Heymann, H. Huppertz, Th. Schleid, *Z. Anorg. Allg. Chem.* 638 (2012) 1119–1122.
- [24] F. Ledderboge, S.J. Metzger, G. Heymann, H. Huppertz, Th. Schleid, *Solid State Sci.* 37 (2014) 164–169.
- [25] S. Schander, *Doctoral Thesis*, Univ. Oldenburg, 2009.
- [26] M. Ben Hamida, M.S. Wickleder, *Z. Anorg. Allg. Chem.* 632 (2006) 2195–2197.
- [27] D.-H. Kang, Th. Schleid, *Z. Anorg. Allg. Chem.* 633 (2007) 1205–1210.
- [28] H. Ben Yahia, U.Ch. Rodewald, R. Pöttgen, *Z. Naturforsch.* 64 b (2009) 896–900.
- [29] H. Ben Yahia, U.Ch. Rodewald, R. Pöttgen, *Z. Naturforsch.* 65 b (2010) 1289–1292.
- [30] H. Ben Yahia, A. Villesuzanne, U.Ch. Rodewald, Th. Schleid, R. Pöttgen, *Z. Naturforsch.* 65 b (2010) 549–555.
- [31] D.-H. Kang, J. Wontcheu, Th. Schleid, *Solid State Sci.* 11 (2009) 299–304.
- [32] (a) R. Hoppe, *Angew. Chem.* 78 (1966) 52–63;
(b) R. Hoppe, *Angew. Chem.* 82 (1970) 7–16;
(c) R. Hoppe, *Angew. Chem.* 92 (1980) 106–121;
(d) R. Hoppe, *Angew. Chem. Int. Ed. Engl.* 5 (1996) 95–106;
(e) R. Hoppe, *Angew. Chem. Int. Ed. Engl.* 9 (1970) 25–34;
(f) R. Hoppe, *Angew. Chem. Int. Ed. Engl.* 9 (1980) 110–125.
- [33] (a) R. Hoppe, *Izv. Jugoslav. Centr. Krist.* 8 (1973) 21;
(b) C.J.M. Rooymans, A. Rabenau (Eds.), *Crystal Structure and Chemical Bonding in Inorganic Chemistry*, Amsterdam, 1975.

- [34] W. Kleber, *Cryst. Res. Tech.* 2 (1967) 13–14.
- [35] A. Neuhaus, *Jb LA Forsch, NRW* (1965) 487–515.
- [36] B.O. Loopstra, H.M. Rietveld, *Acta Crystallogr. B* 25 (1969) 787–791.
- [37] J.O. Sawyer, *J. Inorg. Nucl. Chem.* 34 (1972) 3268–3271.
- [38] K. Binnemans, *Coord. Chem. Rev.* 295 (2015) 1–45.
- [39] B. Lafuente, R.T. Downs, H. Yang, N. Stone, The power of databases: the RRUFF project. In: *Highlights in Mineralogical Crystallography*, T. Armbruster, R.M. Danisi, W. de Gruyter, Berlin, 2015, 1–30, RRUFF ID: R120146.
- [40] B. Lafuente, R.T. Downs, H. Yang, N. Stone, The power of databases: the RRUFF project, in: *Highlights in Mineralogical Crystallography*, T. Armbruster, R.M. Danisi, W. de Gruyter, Berlin, 2015, 1–30, RRUFF ID: R060417.
- [41] B. Lafuente, R.T. Downs, H. Yang, N. Stone, The power of databases: the RRUFF project, in: *Highlights in Mineralogical Crystallography*, T. Armbruster and R. M. Danisi, W. de Gruyter, Berlin, 2015, 1–30, RRUFF ID: R060428.
- [42] (a) G.M. Sheldrick, *Acta Crystallogr. A* 64 (2008) 112–122;
 (b) G.M. Sheldrick, *Acta Crystallogr. A* 69 (2013) 74;
 (c) G.M. Sheldrick, *Acta Crystallogr. C* 71 (2015) 3–8.
- [43] V. Schomaker, R.E. Marsh, *Acta Crystallogr. A* 39 (1983) 819–820.
- [44] R.X. Fischer, E. Tillmanns, *Acta Crystallogr. C* 44 (1988) 775–776.